Received: 30 April 2021 | Revised: 24 May 2021 | Accepted: 25 May 2021

DOI: 10.1002/mdp2.255

SPECIAL ISSUE ARTICLE

WILEY

Energy release as a parameter for fatigue design of additive manufactured metals

Dario Santonocito[1] | **Andrea Gatto**[2] | **Giacomo Risitano**[1]

[1]Department of Engineering, University of Messina, Messina, Italy

[2]Department of Engineering Enzo Ferrari, University of Modena and Reggio Emilia, Modena, Italy

Correspondence
Dario Santonocito, Department of Engineering, University of Messina, Contrada di Dio (S. Agata), 98166 Messina, Italy.
Email: dsantonocito@unime.it

Abstract

Additive manufacturing (AM) is spreading in a wide range of industrial fields. The influence of the printing parameters on the mechanical performance is still an open issue among researchers, particularly when dealing with fatigue loads, which can lead to an unexpected failure. Classical fatigue tests require a large amount of time and materials to be consumed. Compared to the traditional fatigue assessment, the thermographic method (TM) is able to derive in a very rapid way the SN curve and fatigue limit of the material monitoring its energetic release during fatigue tests.

In this work, for the first time, the energetic release during fatigue test has been evaluated in specimens made of AISI 316L, obtained by SLM technique. Compared to literature data, the specimens show premature failure, even at low stress levels, with brittle fracture surfaces. The internal microstructure seems to be strictly related to the energetic release of the material.

KEYWORDS

AISI 316L, fatigue, SLM, thermographic method

1 | INTRODUCTION

Additive manufacturing (AM) technology was created in the 1980s. At first, it was adopted as a rapid prototyping technique,[1] but in the recent years, the demand for real components has been increasing due to their low-weight and low material consumption compared to traditional manufacturing techniques.[2,3] It is of fundamental importance to guarantee mechanical reliability in such components, especially dealing with stresses changing over time. Classical fatigue tests usually require a large amount of material and time in order to obtain a complete SN curve; hence, such procedure is incompatible to a rapid time-to-market for real components. The uncertainty of the AM process parameters, in addition to long test time, may represent a serious economic investment for companies.[4] On the other hand, the development of rapid fatigue assessment methods can significantly reduce time to obtain fatigue behavior of materials. The thermographic method (TM)[5,6] is able to derive in a very rapid and reliable way the SN curve and the fatigue limit of the material monitoring its energetic release during fatigue tests.[7] In 2013, Risitano and Risitano proposed the static thermographic method (STM)[8] as a rapid test procedure to derive the first damage within the material assessing the end of the thermoelastic effect during a static tensile test. These rapid energetic procedures have been widely applied to several classes of material: plain and notched steel specimens under static and fatigue tests,[7–16] laminated composite under tensile static loadings,[17–19] polyethylene under static and fatigue loadings,[20,21] concrete,[22] short glass fiber-

reinforced polyamide composites under static and fatigue loadings,[23,24] steels under high cycle,[7,14,25,26] and very high cycle fatigue regimes.[12,27] More recently, Santonocito applied the STM on 3D-printed PA12 in order to assess damage initiation within the material monitoring the energetic release during a static tensile test.[28]

The aim of the present work is to monitor the energetic release of an AM metal in order to investigate its fatigue life which can be severally affected by building direction, printing parameters and postprocessing treatments.

2 | THE THERMOGRAPHIC METHOD

As observed by La Rosa and Risitano,[5] during a fatigue test, performed at a stress level above the fatigue limit σ_0 of the material and at a given stress ratio R and test frequency f, the temperature trend of engineering materials exhibits three phases (Figure 1A). In the first phase (Phase I), there is a temperature increment until the temperature stabilize at a value equal to ΔT_{st} (Phase II). As the material approaches to fail, temperature experiences a very high further increment (Phase III) till breakage. If the test is performed at stress levels below the fatigue limit, noise or no temperature increment are observed; hence, fatigue limit can be identified in a rapid way as the first stress level for which the stabilization temperature is higher compared to the previous value.[25] For each constant amplitude (CA) fatigue test, it is possible to evaluate the energy parameter Φ as the subtended area of the temperature versus number of cycle curve ($\Delta T - N$). Generally, the higher the applied stress, the higher the stabilization temperature, but the energy parameter could be assumed as material property, given the stress ratio and test frequency. According to the previous observations, it is possible to perform a stepwise fatigue test (Figure 1B), increasing the applied stress level and registering the relative stabilization temperature.[6] As the specimen fail, it is possible to evaluate the energy parameter Φ and assess the number of cycles to failure for each stress level, as the specimen would be stressed at that stress level with CA tests, simply dividing the energy parameter for the different stabilization temperatures and neglecting Phase I and III, usually smaller compared to Phase II. Knowing the $N - \sigma$ values, it is possible to obtain the complete SN curve of the material with a very small number of tests (even three for statistical dispersion).

3 | MATERIALS AND METHOD

The material under study was a stainless steel AISI 316L obtained by selective laser melting (SLM) printing process. Four specimens were printed along the Z direction, according to the ASTM E466 geometry[29] reported in Figure 2A, with the layers perpendicular respect to the loading direction. The specimens were obtained from AISI 316L powder, adopting a laser power of 230 W and a laser scanning speed of 1400 mm/s. The overall printing volume was $110 \times 110 \times 200$ mm^3 with nitrogen atmosphere. Three specimens were tested adopting a stepwise procedure, with

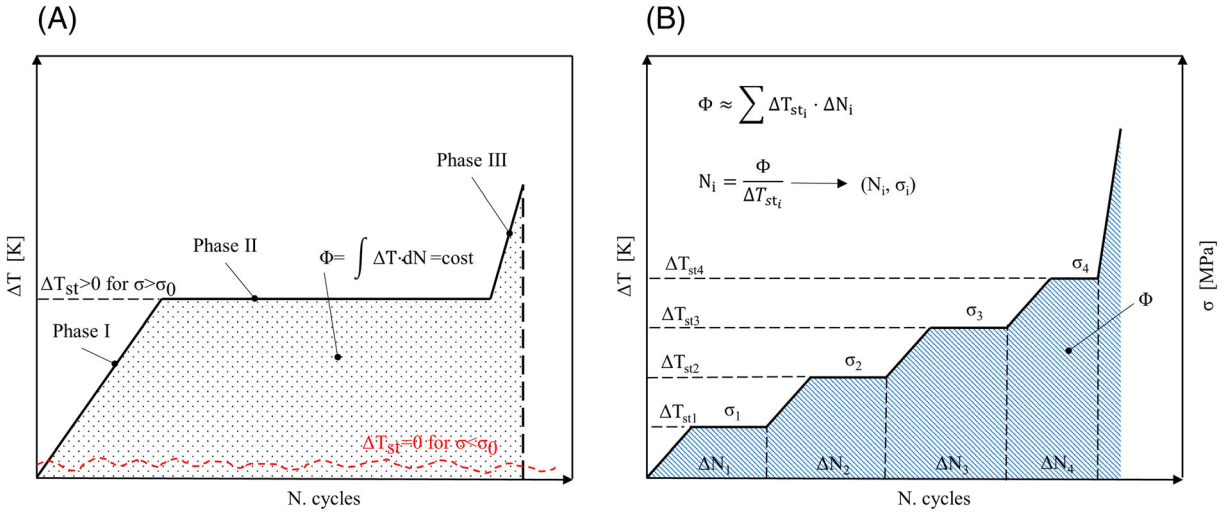

FIGURE 1 Thermographic method: (A) temperature evolution during constant amplitude fatigue test (from 5); (B) stepwise fatigue test to assess the stabilization temperature for each stress level (from 6)

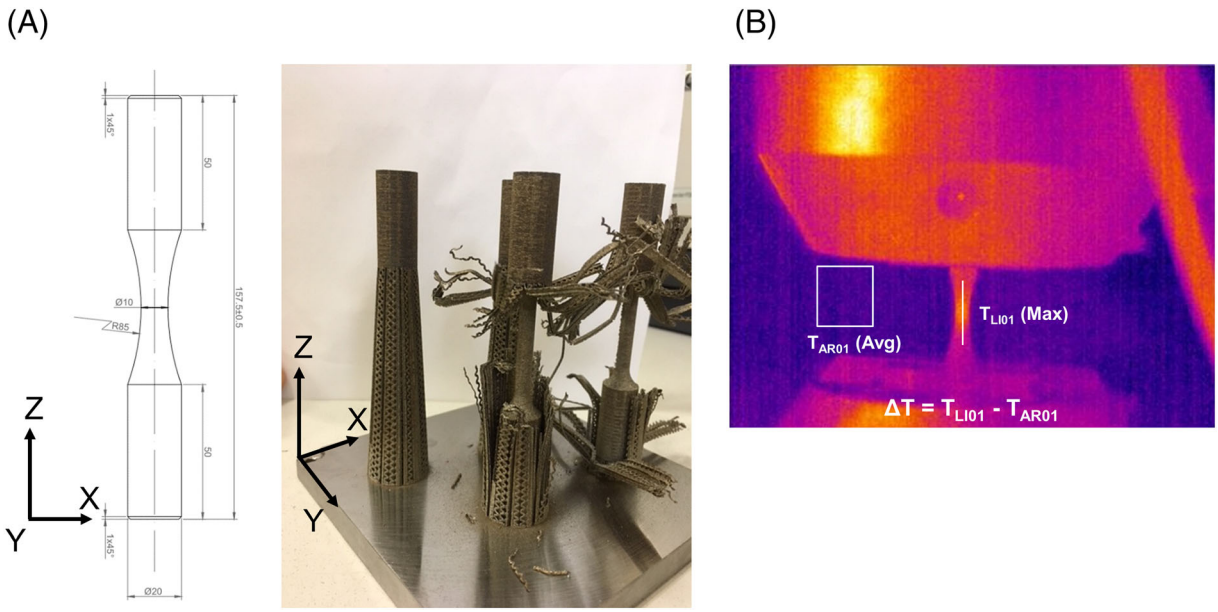

FIGURE 2 (A) Geometry of the tested specimens; (B) thermal measurement areas

stress levels ranging from 80 to 140 MPa ($\Delta\sigma = 10$ MPa, $\Delta N = 10{,}000$), while one specimen was tested with a CA stress level (130 MPa). The stress ratio was set to $R = 0.1$, and the test frequencies were chosen equal to 10 and 20 Hz. All the fatigue tests were performed adopting a servo hydraulic loading machine INSTRON 250 kN, and the specimen superficial temperature was monitored with an infrared camera FLIR A40 (Figure 2B). Room temperature (average value over a rectangular area, T_{AR01}) was subtracted from the specimen temperature (maximum value of the straight line, T_{LI01}), as well as their values at the beginning of fatigue test.

4 | RESULTS AND DISCUSSION

The first three fatigue tests have been performed adopting a stepwise increase of the stress level and monitoring the temperature evolution up to the specimen failure. In Figure 3A,B are reported the temperature trend and the applied stress level versus the number of cycles to failure for a stress ratio of $R = 0.1$ and test frequency $f = 10$ Hz for the first two tested specimens. It is possible to observe how temperature does not experience any significative increment ($\Delta T < 1$ K). Temperature signal is very noisy, and the specimens never reached a stabilization temperature. The only higher temperature increment is noticed prior to the specimen failure. Generally, in common engineering materials, increasing the testing frequency lead to a higher energy release, hence to a higher observed temperature, but for this AM material, doubling the test frequency, from 10 to 20 Hz, does not results in any significative temperature increment (Figure 3C).

The constant amplitude test has been performed at a stress level of 130 MPa with a frequency of 20 Hz. Compared to the stepwise fatigue tests, this specimen shows an early fatigue failure ($N_f = 4313$) with a very noisy temperature signal, lower than 1 K (not reported here for sake of brevity).

In a recent work, Solberg et al[30] tested machined AISI 316L specimens built along Z direction, with stress ratio $R = 0.1$, observing how the fatigue performances of the AM material are severally affected by surface roughness and porosity. In HCF regime, they observed a transition of the failure mechanism: for higher stress levels, failure initiates from internal defect, while for lower stress level, it initiates from superficial defects.

Afkhami et al[31] made a comparison of several AISI 316L specimens obtained with different processing parameters (horizontal, machined vertical, HFMI-treated, and conventional material). They noticed worst fatigue performance of the as-built specimens due to their defects and poor surface quality. On the other hand, adopting different building directions as well as post processing treatment, the fatigue performance of AM AISI 316L is equivalent to the conventional material.

In Figure 4 are reported the fatigue data from the three stepwise fatigue tests (failure stress level vs. number of cycles) and from the CA test with the fatigue data from Solberg et al[30] for vertical machined specimens at $f = 10$ Hz.

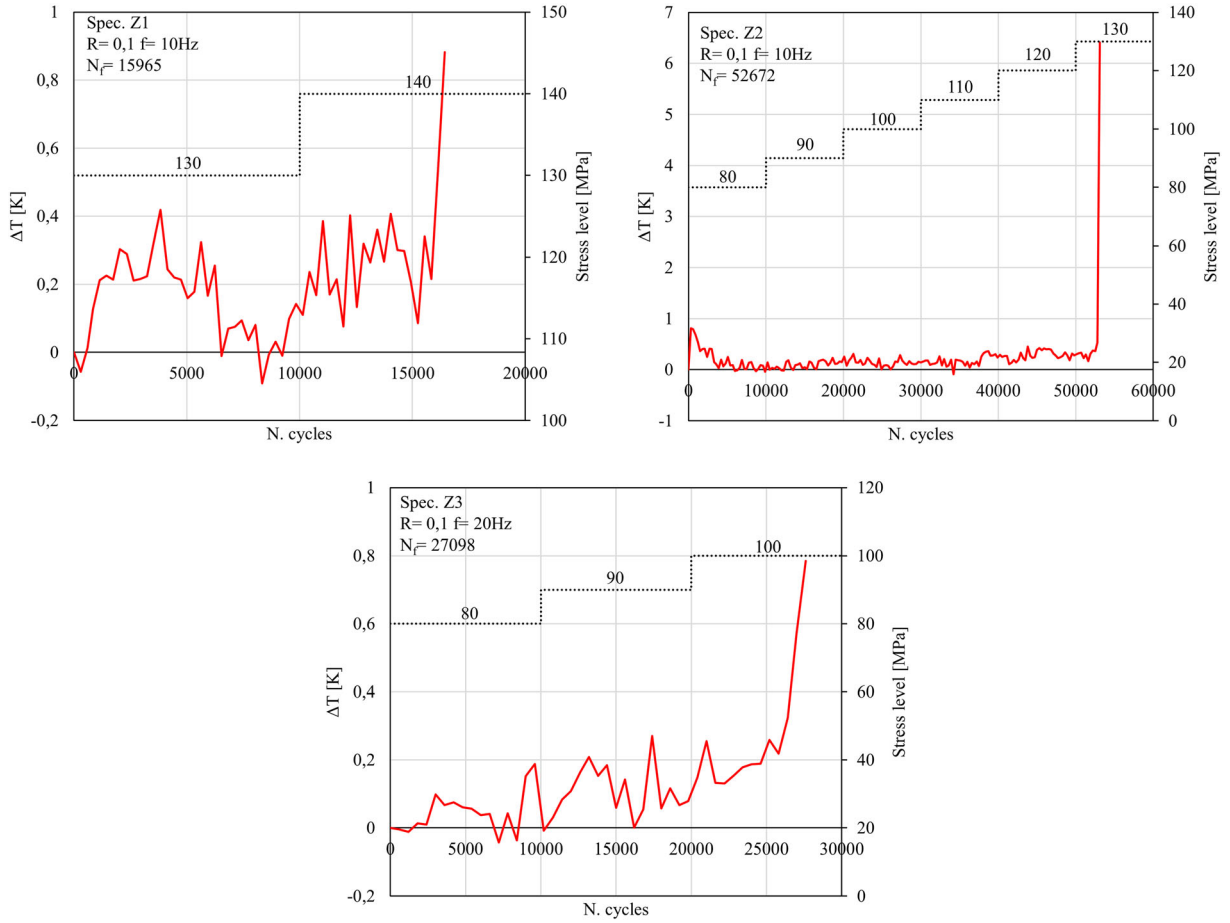

FIGURE 3 Temperature evolution for stepwise fatigue tests

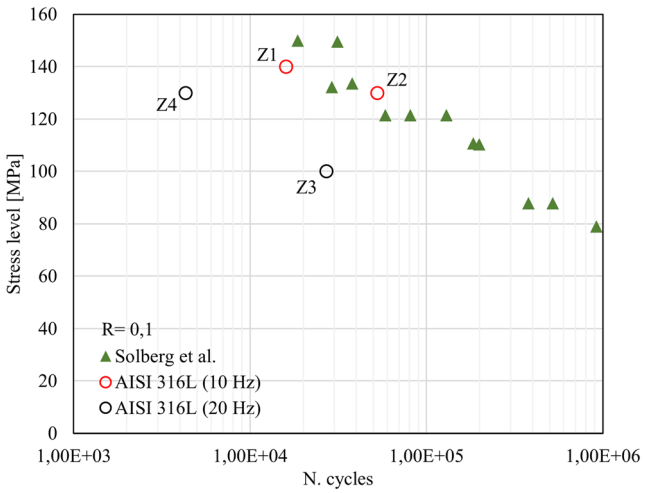

FIGURE 4 Comparison of fatigue life at $R = 0.1$ from Solberg et al[30] and test performed at 10 and 20 Hz

Dealing with the two stepwise fatigue tests performed at 10 Hz (Z1 and Z2, red circles), they fall in the same range of the fatigue tests by Solberg. On the other hand, the stepwise fatigue test Z3 and the CA fatigue test Z4, performed at 20 Hz, exhibit a shorter fatigue life compared to the data of Solberg, suggesting a dependence of the fatigue behavior from the test frequency.

After the fatigue tests, the fracture surfaces of the specimens have been evaluated. All the tested specimens failed in the central section and showed a similar behavior. In Figure 5A are reported the upper and lower fracture surfaces of the specimen Z2, showing a very smoother profile, typical of a brittle failure. It is possible to clearly distinguish the AISI

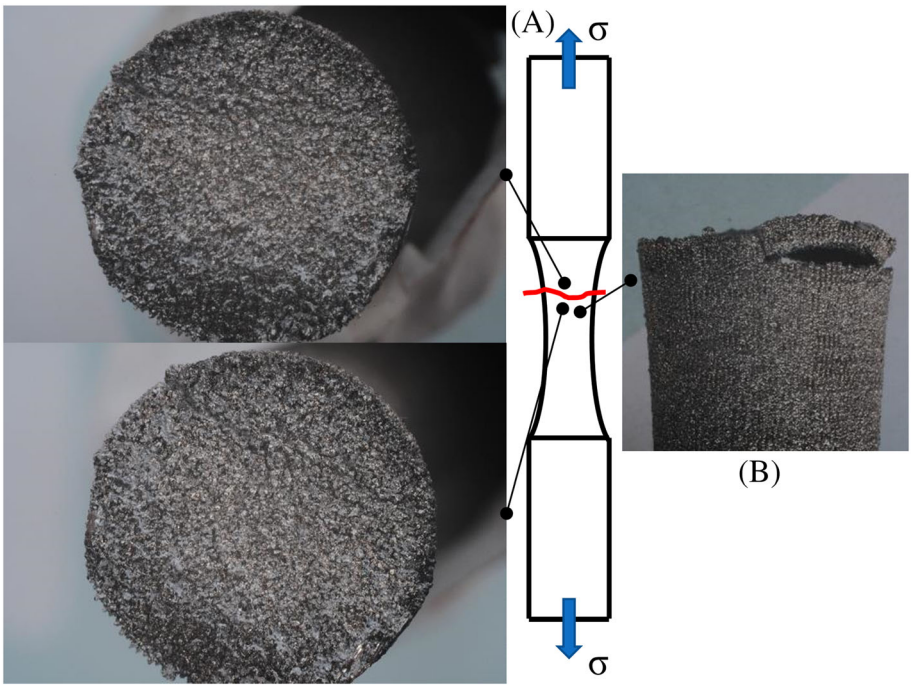

FIGURE 5 Fracture surfaces of the specimen Z2: (A) upper and lower faces; (B) layer debonding respect the loading direction

316L powder adopted in the SLM printing, a laser powder bed fusion (L-PBF) printing technique, while it is difficult to assess the crack initiation site. In Figure 5B, it is possible to observe a debonding of the layer printed along the *Z* direction. This kind of debonding is reasonably responsible for the sudden specimen failure and very low temperature increment during fatigue tests. As observed by Afkhami et al,[31] defects in L-PBF printing tends to elongate perpendicularly to the building direction, and this can lead to higher stress concentration in specimens built along the vertical direction. The normal alignment of the layers respect to the loading direction, with lower fatigue performances compared to horizontal specimens, leads to an easier crack initiation and propagation at these sites.

5 | CONCLUSION

In this work, the energy release of stainless steel AISI 316L specimens, obtained by means of SLM printing process, has been evaluated. The specimens were built along the *Z* direction and were fatigue tested with constant amplitude and stepwise increase of the applied stress level, adopting a stress ratio $R = 0.1$ and test frequency of 10 and 20 Hz. All the tested specimens showed none to very small temperature increment, without reaching a stabilization temperature, and noisy signal compared to the typical temperature trend observed in a wide range of engineering materials. Fatigue data have been compared with the ones present in literature for the same test conditions showing worst fatigue performances compared to different building directions and post processing treatments. Internal microstructure and surface quality are strictly related to the printing parameters and can severally affect fatigue performances of AM metals. Further study on the energy release of these materials should be performed in order to provide an easy and rapid way to assess fatigue behavior of AM devices.

CONFLICT OF INTEREST

The authors declare no conflict of interest.

DATA AVAILABILITY STATEMENT

The data that support the findings of this study are available from the corresponding author upon reasonable request.

ORCID

Dario Santonocito https://orcid.org/0000-0002-9709-9638

REFERENCES

1. Weller C, Kleer R, Piller FT. Economic implications of 3D printing: market structure models in light of additive manufacturing revisited. *Int J Prod Econ*. 2015;164:43-56.
2. Ngo TD, Kashani A, Imbalzano G, Nguyen KTQ, Hui D. Additive manufacturing (3D printing): a review of materials, methods, applications and challenges. *Compos Part B Eng*. 2018;143:172-196.
3. Galati M, Calignano F, Viccica M, Iuliano L. Additive manufacturing redesigning of metallic parts for high precision machines. *Crystals*. 2020;10(3):1-22.
4. Piscopo G, Salmi A, Atzeni E, et al. On the effect of deposition patterns on the residual stress, roughness and microstructure of AISI 316L samples produced by directed energy deposition. In: Almeida HA, Vasco JC, eds. *Progress in Digital and Physical Manufacturing*. Cham: Springer International Publishing; 2020:206-212.
5. La Rosa G, Risitano A. Thermographic methodology for rapid determination of the fatigue limit of materials and mechanical components. *Int J Fatigue.* 2000;22(1):65-73.
6. Fargione G, Geraci A, La Rosa G, Risitano A. Rapid determination of the fatigue curve by the thermographic method. *Int J Fatigue.* 2002;24(1):11-19.
7. Corigliano P, Cucinotta F, Guglielmino E, Risitano G, Santonocito D. Fatigue assessment of a marine structural steel and comparison with thermographic method and static thermographic method. *Fatigue Fract Eng Mater Struct*. 2020;43(4):734-743.
8. Risitano A, Risitano G. Determining fatigue limits with thermal analysis of static traction tests. *Fatigue Fract Eng Mater Struct*. 2013; 36(7):631-639.
9. Risitano G, Clienti C. Experimental study to verify the fatigue limit found by thermal analysis of specimen surface in mono axial traction test. *Key Eng Mater*. 2012;488–489:795-798.
10. Risitano A, Fargione G, Guglielmino E. Definition of the linearity loss of the surface temperature in static tensile tests. *Frat Ed Integrita Strutt.* 2014;30:201-210.
11. Ricotta M, Meneghetti G, Atzori B, Risitano G, Risitano A. Comparison of experimental thermal methods for the fatigue limit evaluation of a stainless steel. *Metals (Basel).* 2019;9:677.
12. Plekhov O, Naimark O, Semenova I, Polyakov A, Valiev R. Experimental study of thermodynamic and fatigue properties of submicrocrystalline titanium under high cyclic and gigacyclic fatigue regimes. *Proc Inst Mech Eng Part C J Mech Eng Sci*. 2014;229:1271-1279.
13. Amiri M, Khonsari MM. Life prediction of metals undergoing fatigue load based on temperature evolution. *Mater Sci Eng a*. 2010;527(6): 1555-1559.
14. Amiri M, Khonsari MM. Rapid determination of fatigue failure based on temperature evolution: fully reversed bending load. *Int J Fatigue*. 2010;32(2):382-389.
15. Rigon D, Ricotta M, Meneghetti G. Analysis of dissipated energy and temperature fields at severe notches of AISI 304L stainless steel specimens. *Frat Ed Integrita Strutt*. 2019;13:334-347.
16. Corigliano P, Cucinotta F, Guglielmino E, Risitano G, Santonocito D. Thermographic analysis during tensile tests and fatigue assessment of S355 steel. *Procedia Struct Integr*. 2019;18:280-286.
17. Colombo C, Vergani L, Burman M. Static and fatigue characterisation of new basalt fibre reinforced composites. *Compos Struct*. 2012; 94(3):1165-1174.
18. Palumbo D, De Finis R, Demelio PG, Galietti U. Early detection of damage mechanisms in composites during fatigue tests. In: Zehnder AT, Carroll J, Hazeli K, et al., eds. *Fracture, Fatigue, Failure and Damage Evolution*. Vol.8. Cham: Springer International Publishing; 2017:133-141.
19. Vergani L, Colombo C, Libonati F. A review of thermographic techniques for damage investigation in composites. *Frat Ed Integrita Strutt*. 2014;8:1-12.
20. Risitano G, Guglielmino E, Santonocito D. Evaluation of mechanical properties of polyethylene for pipes by energy approach during tensile and fatigue tests. In: *Procedia Structural Integrity*. Vol.13. Elsevier B.V.; 2018:1663-1669.
21. Risitano G, Guglielmino E, Santonocito D. Energetic approach for the fatigue assessment of PE100. *Procedia Struct Integr*. 2020;26: 306-312.
22. Cucinotta F, D'Aveni A, Guglielmino E, Risitano A, Risitano G, Santonocito D. Thermal emission analysis to predict damage in specimens of high strength concrete. *Frat Ed Integrita Strutt.* 2021;15:258-270.
23. Crupi V, Guglielmino E, Risitano G, Tavilla F. Experimental analyses of SFRP material under static and fatigue loading by means of thermographic and DIC techniques. *Compos Part B Eng*. 2015;77:268-277.
24. Santonocito D. Numerical and experimental evaluation of the energetic release during static tensile tests on short fiber reinforced composite material. *IOP Conf Ser Mater Sci Eng*. 2021;1038(1):012059.
25. Curà F, Curti G, Sesana R. A new iteration method for the thermographic determination of fatigue limit in steels. *Int J Fatigue*. 2005; 27(4):453-459.
26. Meneghetti G, Ricotta M, Atzori B. A synthesis of the push-pull fatigue behaviour of plain and notched stainless steel specimens by using the specific heat loss. *Fatigue Fract Eng Mater Struct*. 2013;36(12):1306-1322.
27. Crupi V, Epasto G, Guglielmino E, Risitano G. Thermographic method for very high cycle fatigue design in transportation engineering. *Proc Inst Mech Eng Part C J Mech Eng Sci*. 2015;229(7):1260-1270.
28. Santonocito D. Evaluation of fatigue properties of 3D-printed polyamide-12 by means of energy approach during tensile tests. *Procedia Struct Integr*. 2020;25:355-363.

29. ASTM. E466 - Practice for conducting force controlled constant amplitude axial fatigue tests of metallic materials. 2015.
30. Solberg K, Guan S, Razavi SMJ, Welo T, Chan KC, Berto F. Fatigue of additively manufactured 316L stainless steel: the influence of porosity and surface roughness. *Fatigue Fract Eng Mater Struct*. 2019;42(9):2043-2052.
31. Afkhami S, Dabiri M, Piili H, Björk T. Effects of manufacturing parameters and mechanical post-processing on stainless steel 316L processed by laser powder bed fusion. *Mater Sci Eng A*. 2021;802:140660.

How to cite this article: Santonocito D, Gatto A, Risitano G. Energy release as a parameter for fatigue design of additive manufactured metals. *Mat Design Process Comm*. 2021;e255. https://doi.org/10.1002/mdp2.255